

A molecular view of Tanner's law: molecular dynamics simulations of droplet spreading

By G. HE AND N. G. HADJICONSTANTINO[†]

Mechanical Engineering Department, 77 Massachusetts Avenue, Massachusetts
Institute of Technology, Cambridge, MA 02139, USA

(Received 9 July 2003 and in revised form 24 September 2003)

By truncating the range of van der Waals forces in our molecular dynamics model we reduce the lengthscale and timescale gap between the outer (wedge) and inner (precursor) regions in droplet spreading simulations. This results in a molecular model which combines atomic-scale resolution with the ability to capture large-scale behaviour as manifested by the Tanner spreading law. Our results show that Tanner's law can be recovered, even if van der Waals effects and the resulting precursor film are limited to distances of the order of three atomic diameters from the substrate. In other words, removal of the singularity is not necessary up to a few atomic diameters from the contact line. The very good quantitative agreement with theory and experiments suggests that the original precursor theory of de Gennes can be generalized to precursors of molecular thickness in which flow is not characterized by the continuum (Stokes) model. Gravity current simulations are also in excellent agreement with the theory of Huppert and recent experimental results showing lubrication scalings at small capillary numbers.

1. Introduction

The subject of contact-line motion (Dussan V. 1979) has received significant attention over the last three decades due to both the large number of practical applications in which it appears and the interesting scientific challenges it poses. The most challenging, perhaps, aspect of the problem is the removal of a divergence in the stress at the contact line predicted by continuum theory (Huh & Scriven 1971). This failure of continuum theory has prompted researchers to use various molecular approaches such as molecular-kinetic modelling (Blake & Haynes 1969; Cazabat *et al.* 1997), molecular dynamics simulations (Koplik, Banavar & Willemsen 1989; Thompson & Robbins 1989; Yang, Koplik & Banavar 1991; De Coninck *et al.* 1995; D'Ortona *et al.* 1996; Hadjiconstantinou 1999) and Monte Carlo simulations (Milchev, Milchev & Binder 2002), to capture the spreading dynamics in the contact-line vicinity. These studies have been useful for providing information on the local fluid behaviour, and in the case of certain liquid–liquid flows where disjoining pressure effects are not important, for making quantitative connections to large-scale hydrodynamic behaviour (Thompson & Robbins 1989; Hadjiconstantinou 1999).

In the case of liquid–gas systems, molecular simulations have been limited to the study of nanoscopic droplets. These droplets are too small to exhibit the macroscopically observed Tanner spreading law (Voinov 1976; Tanner 1979) since

[†] Author to whom correspondence should be addressed: ngh@mit.edu

their characteristic lengthscales fall well within the distances where van der Waals forces are important. As a result, molecular dynamics simulations to date have only been able to provide information on terraced spreading of nanoscale droplets (De Coninck *et al.* 1995; D’Ortona *et al.* 1996; Cazabat *et al.* 1997) which exhibit diffusive-like dynamics (Abraham, Cuerno & Moro 2002).

The objective of this paper is to perform molecular dynamics simulations of fully wetting droplets spreading under capillary action which capture the macroscopically observed Tanner law. One of the leading theories of this behaviour is that of de Gennes and co-workers (Hervet & de Gennes 1984; de Gennes 1985) which removes the shear stress singularity at the contact line through a precursor film.† As we explain below, our approach was inspired by this theory; the resulting agreement between our results and macroscopic predictions thus validates the physical premise of this approach. In fact, our results imply the validity of a more general theory which includes non-continuum precursors.

According to the theory by de Gennes and co-workers, fully wetting droplets exhibit two regions where different dynamical processes dominate, namely the region where surface tension forces balance viscous forces (which we will refer to as the ‘wedge region’) and the precursor film where forces due to disjoining pressure are balanced by viscosity. Our approach utilizes this fact to obtain molecular simulations which capture both the outer macroscopic behaviour and the molecular behaviour at the contact line. This is achieved by cutting off the wall–fluid interaction at a distance r_c and supplying no long-range correction for this interaction. This ensures that at heights above r_c van der Waals forces from the substrate, and hence disjoining pressure effects, do not play a role. In some sense, this approach reduces the region where van der Waals effects are important in order to reduce the lengthscale and timescale gap between the molecular-scale contact-line physics and the outer-scale physics, and make the observation of both phenomena possible within the same model. Such an approach is necessary since a brute force study of Tanner’s law using molecular dynamics would have been well beyond our computational capabilities; typical droplet sizes amenable to simulation are of the order of the minimum thickness of the adiabatic precursor film (Joanny & de Gennes 1986), which is itself significantly smaller than the range of van der Waals forces.

Owing to its small transverse dimension (less than three atomic diameters), flow in the precursor film observed in our simulation is not described by the Stokes flow/disjoining pressure model. This, however, should not be seen as a disadvantage for two reasons. First, a quantitative verification of de Gennes’ predictions for large-scale droplets involving a continuum precursor has been completed recently (Kavehpour, Ovrn & McKinley 2003). Second, our results serve to demonstrate that de Gennes’ theory is in fact more generally applicable than originally believed, since it also captures the emergence of Tanner’s law from the matching of the wedge region to a *non-continuum* precursor region. Our results show that Tanner behaviour can still be obtained when the wedge region extends to distances of three atomic diameters from the contact line.

Behaviour that is close to Tanner’s law was recently reported by Milchev *et al.* (2002) who used a simple Monte Carlo model of droplet spreading. The origin of the observed behaviour is not clear since the Monte Carlo approach is expected to

† Although a singularity still exists at the end of the precursor film, this theory is successful in accounting for the total dissipation in the spreading system, albeit through the use of conjectures, by considering only the droplet and the early part of the precursor.

model correctly equilibrium systems or systems approaching equilibrium and should, strictly speaking, not be used for non-equilibrium flows. Additionally the system used by Milchev *et al.* (128 chains of 32 beads) is so small that should, under normal circumstances, be dominated by van der Waals forces and exhibit terraced spreading. The observed behaviour may be due to the simplified wall–fluid interaction potential used in the above study (the wall was structureless and the only force between the wall and the fluid was due to a shifted van der Waals potential) which may have resulted in a sufficiently reduced wall–fluid interaction.

In the next section we describe our simulation method and in §3 we present our simulation results. We finish with our conclusions in §4.

2. Molecular simulations

We performed molecular dynamics (Allen & Tildesley 1987) simulations of droplet spreading on a molecular wall. In order to minimize the computational cost of our simulations, two-dimensional (cylindrical) droplets in the (x, z) -plane were considered; this was achieved by making the simulation in the y -direction thin and periodic. The molecular motion and dynamics was, of course, three-dimensional. A Langevin thermostat (He & Robbins 2001) was used to maintain the substrate at a constant temperature of $T = 0.793\epsilon/k_B$, where k_B is Boltzmann's constant.

The spreading droplet consists of 6799 linear polymeric chain molecules. Each chain contains four monomers interacting through a Lennard–Jones potential

$$V_{LJ}(r) = 4\epsilon \left[\left(\frac{\sigma}{r} \right)^{12} - \left(\frac{\sigma}{r} \right)^6 \right], \quad (2.1)$$

where ϵ and σ are the Lennard–Jones characteristic energy and length scales. A characteristic molecular timescale can be defined as $t_{LJ} = \sqrt{m\sigma^2/\epsilon}$, where m is the mass of a fluid monomer. Neighbouring monomers on the chain interact with an additional FENE (finitely extensible nonlinear elastic) potential,

$$V_{FENE}(r) = -\frac{1}{2}kR_0^2 \ln[1 - (r/R_0)^2], \quad (2.2)$$

where $k = 30\epsilon\sigma^{-2}$ and $R_0 = 1.5\sigma$. These values have been widely used in previous simulation studies of polymeric systems (He & Robbins 2001). At the temperature of the simulation, the polymer droplet is in the fluid state and there is almost no vapour present. The droplet equilibrium density is $\rho = 0.9\sigma^{-3}$.

The wall is made of four layers of atoms which are explicitly simulated. Wall atoms are tethered to lattice sites of an FCC lattice with its (111) surface facing the fluid. At the wall density, $\rho_w = 0.81\sigma^{-3}$, the nearest neighbour distance of the lattice is $d_{nn} = 1.2\sigma$ and the thickness of four layers of wall atoms is larger than 3σ , the cut-off distance of the wall–fluid interaction. The tethering potential is also of the FENE type with $k_w = 460\epsilon\sigma^{-2}$ and $R_{w0} = 15\sigma$. The value of k_w is chosen according to the Lindeman criterion for no melting (He & Robbins 2001) which requires the root-mean-square distance of the oscillating wall atoms around their tethering points to be much smaller than the lattice constant.

The wall atoms interact with fluid monomers through a Lennard–Jones potential cut-off at $r_c = 3.0\sigma$. The wall–fluid interaction parameters ($\epsilon_{fw} = 4.0\epsilon$ and $\sigma_{fw} = 1.0\sigma$) were chosen such that polymeric fluid completely wets the substrate but otherwise arbitrarily. This interaction is similar to the one used and extensively studied by De Coninck *et al.* (1995), D'ortona *et al.* (1996) and Koplik & Banavar (2000). The

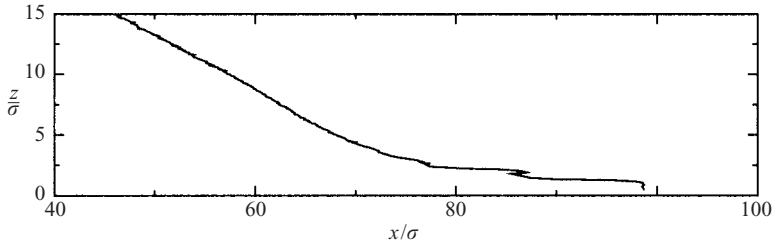


FIGURE 1. Averaged droplet shape over a period of $4000t_{LJ}$. The shape shows the wedge region where surface tension balances viscous forces and the precursor region where the excess free energy associated with the uncompensated Young force is dissipated (de Gennes 1985).

spreading fluid exhibits layering close to the wall, similar to that observed by De Coninck *et al.* (1995) and D’Ortona *et al.* (1996).

The droplet has an initial contact angle $\theta_0 \sim 30^\circ$, an initial radius $R_0 \sim 67\sigma$ and a height $h_0 \sim 30\sigma$. This angle represents a compromise between computational cost and the need for a small contact angle, an inherent approximation in the version of Tanner’s law studied here. Smaller angles would require very large systems since the droplet height needs to be at least of order 20σ – 30σ for a non-negligible wedge region to be present, especially at late times.

We have used a gravity-driven Poiseuille flow to measure the viscosity of our spreading fluid. At the average density and temperature of our simulation the viscosity is measured from the curvature of the velocity profile. We found that the viscosity of the polymer droplet is $\mu = (2.6 \pm 0.2)\varepsilon\sigma^{-3}t_{LJ}$. The surface tension of the droplet is measured by calculating the stress tensor of an equilibrium cylindrical polymer droplet suspended in vacuum (since there is no vapour). The surface tension, γ , can be evaluated using the Laplace equation $\gamma = \Delta p R$, where Δp is the difference between pressure inside a droplet and the pressure of the vapour (in our case zero). A second approach for measuring the surface tension is through the integration of the difference between the longitudinal and tangential components of the stress tensor (Rowlinson & Widom 1982). Provided that the radius of the droplet is large (compared to the molecular diameter),

$$\gamma \approx \int_0^\infty (P_\perp - P_\parallel) dr, \quad (2.3)$$

where r is the radial coordinate. Both methods give an estimate of $\gamma = (1.1 \pm 0.1)\varepsilon\sigma^{-2}$.

The droplet shape is extracted from our simulation data by scanning the local fluid density. The latter is calculated in two-dimensional bins of approximate linear size 5σ in the scanning direction and 1σ in the normal to the scanning direction. The droplet boundary is defined as the location where the local fluid density first drops to half of that inside the droplet. Our tests show that this algorithm provides a very good description of the droplet shape for both horizontal and vertical scanning.

3. Simulation results

3.1. Capillary-driven flow

Figure 1 shows the average shape of the spreading droplet in the contact-line vicinity. The averaging was performed over a period of $4000t_{LJ}$ during which the droplet shape changes little. The figure shows the wedge region of the droplet as well as the

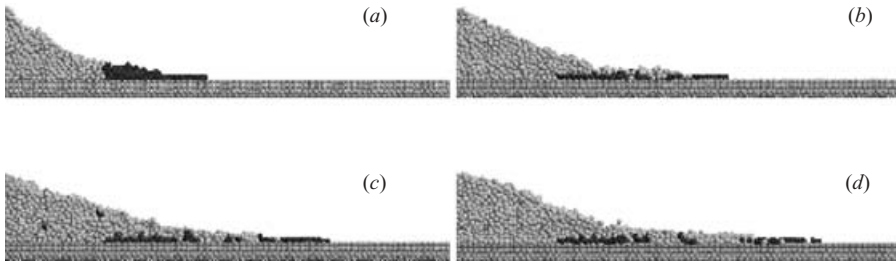


FIGURE 2. Snapshots of the droplet spreading process at (a) $t/t_{LJ} = 5000$, (b) 10 000, (c) 15 000, (d) 20 000. Particles in the precursor region in (a) are marked with a dark colour such that their subsequent motion can be tracked. The caterpillar-type motion first reported by Dussan V. & Davis is observed, as well as slipping motion close to the tip of the precursor.

precursor film. The precursor is very thin – of the order of three molecular layers at the contact line and proceeds to thin to a monomolecular layer at the leading edge. The figure also shows that the wedge approximation is well satisfied, thus simplifying the definition of the apparent contact line location. Our results involving the contact angle are insensitive to the exact location of its measurement in the height range $z = [3.1-7]\sigma$.

The fluid motion inside the droplet in the contact-line vicinity is described by the four snapshots of the spreading process shown in figure 2. In this figure, the atoms forming the precursor at some initial time are labelled by a dark color. By tracking the relative motion of these molecules we can see that the contact line advances in the caterpillar-like motion also observed in macroscopic experiments by Dussan V. & Davis (1974), while the front of the precursor layer is slipping along the substrate.

3.1.1. Tanner's law

We have used two independent methods to quantify the spreading characteristics of the droplets. In the first approach, we examine the time evolution of the radius (half-length in two dimensions) of the droplet, which is expected to follow the form

$$R \propto (t - t_0)^\beta, \quad (3.1)$$

if the droplet spreads according to Tanner's Law $dR/dt \sim \theta^m$. In the above equation β can be related to m by $\beta = 1/(2m + 1)$ (Ehrhard & Davis 1991).

The radius of the droplet (in two dimensions), R , is defined from the droplet centreline to the apparent contact line, that is the precursor film is excluded. This is a subtle distinction, usually omitted in large-scale studies where the precursor length is small and usually not visible. We have found the spreading rate based on R , that is the droplet spreading rate, to be sensitive to the addition of a long-range correction to the interaction between the wall and the fluid in the long time limit (for details on this correction see Israelachvili 1991). On the other hand, we find that the addition of a long-range correction has a small effect on the spreading rate at short times when that is measured at the precursor tip, in agreement with previous work (De Coninck *et al.* 1995; D'Ortona *et al.* 1996; Koplik & Banavar 2000). This observation can be explained by the fact that at short times the droplet motion is dominated by the precursor layer motion (in figure 3 $dR/dt \approx 0$ at short times) which is not sensitive to long-range forces.

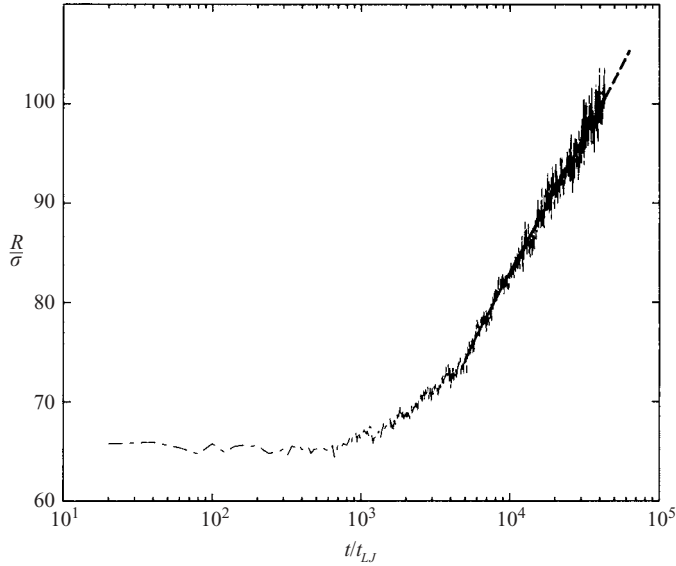


FIGURE 3. Droplet radius (to contact line) as a function of time. The solid line (dashed beyond the range of numerical data) shows the best fit $R \propto (t - t_0)^{0.118}$ at later (hydrodynamic) times.

We fit our simulation data by searching for a range of values of t_0 that minimize the target function,

$$I(t_0) = \sum_i [\ln R_i - \ln \alpha(t_0) - \beta(t_0) \ln(t_i - t_0)]^2, \quad (3.2)$$

where $\alpha(t_0)$ and $\beta(t_0)$ are linear regression fitting parameters for $\ln R_i$ and $\ln(t_i - t_0)$ with t_0 fixed. A similar power law is obtained by looking at even later times and ignoring t_0 . From our fit we find $\beta = 0.118 \pm 0.03$, which is in good agreement with the theoretically expected value of $1/7$. Figure 3 shows the simulation result and our best fit to this data.

In figure 4 we plot the contact angle versus the capillary number, $Ca = \mu U / \gamma$, where $U = dR/dt$ is the contact-line speed. Both quantities were measured as averages (to reduce statistical fluctuations) over small time segments ($O(1000t_{L,J})$) during which we assume that they change very little. The averaging procedure we used is as follows. Droplet configurations are recorded every $20t_{L,J}$ and the algorithm described in §2 is used to extract the droplet boundary. Assuming that the droplet front does not change much during this time period and that it only drifts with the contact-line velocity, we can shift all droplet shapes back to a reference position, that is, we observe the droplet in the moving frame of the contact line. The shifted shapes are then averaged over time and an average contact angle is extracted by linear regression on the averaged droplet shape. We found that this method provides significantly less-fluctuating estimates for the contact angle compared to averaging of the instantaneous contact angles. The contact-line velocity is calculated by differentiating a smoothed version of the droplet radius–time relation.

The data are described by the following fit:

$$\theta = 2.7Ca^{0.29}, \quad (3.3)$$

which is in very good agreement with previous data from experimental studies on

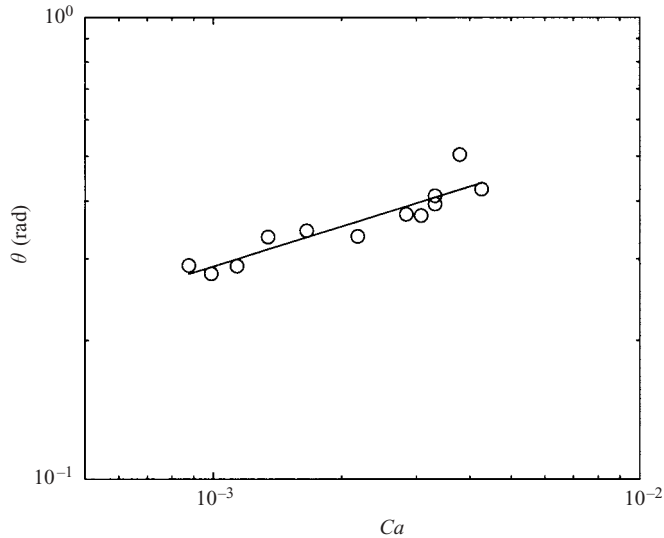


FIGURE 4. Dynamic contact angle as a function of the capillary number in capillary-driven spreading.

macroscopic droplets (Kavehpour, Ovryn & McKinley 2003) as well as theoretical predictions (see Eggers & Stone 2003 and Kavehpour 2003).

The above two independent measurements show that Tanner's law is recovered in droplets with heights as small as 20 molecular diameters, as long as van der Waals effects are limited to within 3σ of the substrate. Smaller droplets with heights less than 15 molecular diameters did not exhibit this behaviour.

3.2. Gravity-driven droplets

We also performed simulations of gravity-driven droplets by adding a body force g acting on the fluid in the direction parallel to the substrate (x -direction). The lack of a force normal to the substrate is consistent with theoretical analyses (Huppert 1982; Troian *et al.* 1989) where hydrostatic effects are neglected.

In this limit, according to Huppert (1982), the droplet can be divided into two regions. In the long tail region in which a Bond number $Bo = \rho g x_N^2 / \gamma$ is much larger than 1, surface tension effects are negligible and a balance between gravity and viscosity yields a similarity solution for the droplet shape $h = h(x, t)$

$$h = (\nu/g)^{1/2} x^{1/2} t^{-1/2}, \quad x_N = (9A^2 g / 4\nu)^{1/3} t^{1/3} \quad (3.4)$$

where $\nu = \mu/\rho$ is the kinematic viscosity, A is the droplet cross-sectional area

$$A = \int_0^{x_N(t)} h(x, t) dx \quad (3.5)$$

and $x_N(t)$ is the location where the droplet ends abruptly through the smoothing effects of surface tension. In this second region, a quasi-steady solution in a frame moving with the contact line at $x_N(t)$ leads to an approximate similarity solution of the form

$$h = h_N(t)H(\xi), \quad H \rightarrow \left(\frac{64}{15}\right)^{1/4} \xi^{3/4} \text{ as } \xi \rightarrow 0, \quad (3.6)$$

where $h_N = h(x_N)$ and $\xi = (\rho g / (\gamma h_N))^{1/3} (x_N - x)$.

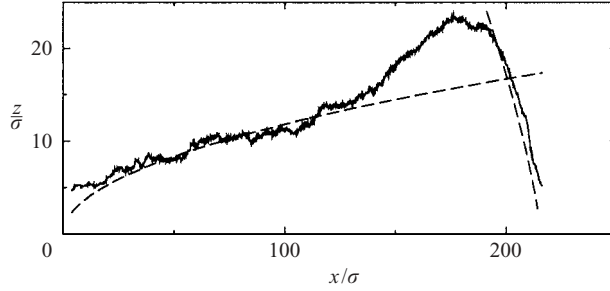


FIGURE 5. Droplet shape in gravity-driven flow. The dashed lines denote the theoretical predictions of Huppert.

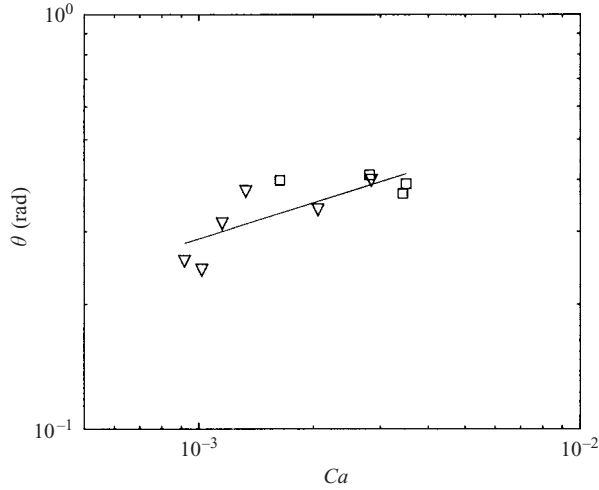


FIGURE 6. Dynamic contact angle as a function of the capillary number. The square symbols denote $g = 0.00005\sigma/t_{LJ}^2$ and triangles denote $g = 0.00001\sigma/t_{LJ}^2$.

Figure 5 shows a comparison between the instantaneous droplet shape and the theoretical predictions of Huppert. It is remarkable that both shapes are in very good agreement with the molecular results, and in particular solution (3.6) which is only approximate (Troian *et al.* 1989; Goodwin & Homsy 1991). Figure 6 shows the dynamic contact angle plotted as a function of the capillary number for small values of the gravity parameter. The data can be fitted by a power law of the form

$$\theta \propto Ca^{0.29}. \quad (3.7)$$

This is in very good agreement with data from a recent experimental study on macroscopic droplets (Kavehpour 2003) which showed that for sufficiently small capillary numbers ($Ca < 0.01$) a lubrication scaling of $Ca^{1/3}$ is observed (Goodwin & Homsy 1991).

4. Conclusions

In this paper we have shown that by judicious choice and consistent implementation of the simulation cut-off distance we can perform quantitative numerical droplet spreading experiments using a molecular dynamics approach. Our approach provides

an opportunity for simultaneous probing at small distances from the contact line while offering comparable resolution at the problem outer scale. This allows the validation of well-known results such as Tanner's law using molecular methods, combined with the ability to probe the dynamics of contact lines at a very fine level of detail and very small scales. Our results for both capillary-driven spreading and gravity currents have been found to be in agreement with previous theoretical and experimental studies using more than one independent test.

Our simulations show that the wedge region in Tanner's law can extend up to distances of the order of three atomic diameters from the contact line before removal of the singularity is necessary. Finally, it appears that de Gennes' wetting theory can be generalized to precursors that are thinner than the minimum equilibrium thickness for which adiabatic precursors exist (Joanny & de Gennes 1986). In our work this precursor is very thin (of the order of a few molecular layers) and lies in the non-continuum regime where the Stokes approximation is not expected to be valid.

The authors are indebted to Professors Anette Hosoi, Pirouz Kavehpour and Gareth McKinley for useful comments and discussions and for making their experimental results available before publication. This work was supported by the Singapore-MIT alliance.

REFERENCES

- ABRAHAM, D. B., CUERNO, R. & MORO, E. 2002 Microscopic model for thin film spreading. *Phys. Rev. Lett.* **88**, 206101.
- ALLEN, M. P. & TILDESLEY, D. J. 1987 *Computer Simulation of Liquids*. Clarendon.
- BLAKE, T. D. & HAYNES, J. M. 1969 Kinetics of liquid/liquid displacement. *J. Colloid Interface Sci.* **30**, 421–423.
- CAZABAT, A. M., VALIGNAT, M. P., VILLETTE, S., DE CONINCK, J. & LOUCHE, F. 1997 The mechanism of spreading: a microscopic description. *Langmuir* **13**, 4754–4757.
- DE CONINCK, J., D'ORTONA, U., KOPLIK, J. & BANAVAR, J. R. 1995 Terraced spreading of chain molecules via molecular dynamics. *Phys. Rev. Lett.* **74**, 928–931.
- D'ORTONA, U., DE CONINCK, J., KOPLIK, J. & BANAVAR, J. R. 1996 Terraced Spreading mechanisms for chain molecules. *Phys. Rev. E* **53**, 562–569.
- DUSSAN V., E. B. 1975 On the spreading of liquids on solid surfaces: static and dynamic contact lines. *Annu. Rev. Fluid Mech.* **11**, 371–400.
- DUSSAN V., E. B. & DAVIS, S. H. 1974 On the motion of a fluid-fluid interface along a solid surface. *J. Fluid Mech.* **65**, 71–95.
- EGGERS, J. & STONE, H. A. 2003 Characteristic lengths at moving contact lines for a perfectly wetting fluid: the influence of speed on the dynamic contact angle. *J. Fluid. Mech.* (Submitted).
- EHRHARD, P. & DAVIS, S. H. 1991 Non-isothermal spreading of liquid drops on horizontal plates. *J. Fluid Mech.* **229**, 365–388.
- DE GENNES, P. G. 1985 Wetting: statics and dynamics. *Rev. Mod. Phys.* **57**, 827–863.
- GOODWIN, R. & HOMSY, G. M. 1991 Viscous flow down a slope in the vicinity of a contact line. *Phys. Fluids* **3**, 515–528.
- HADJICONSTANTINO, N. G. 1999 Combining atomistic and continuum simulations of contact-line motion. *Phys. Rev. E* **59**, 2475–2478.
- HE, G. & ROBBINS, M. O. 2001 Simulations of the static friction due to adsorbed molecules. *Phys. Rev. B* **64**, 035413.
- HERVET, H. & DE GENNES, P. G. 1984 Physique des surfaces et des interfaces. *C. R. Acad. Sci. Paris* **299**, 499–503.
- HUH, C. & SCRIVEN, L. E. 1971 Hydrodynamic model of steady movement of a solid/liquid/fluid contact line. *J. Colloid Interface Sci.* **35**, 85–101.
- HUPPERT, H. E. 1982 Flow and instability of a viscous current down a slope. *Nature* **300**, 427–429.
- ISRAELACHVILI, J. 1991 *Intermolecular and Surface Forces*. Academic.

- JOANNY, J. F. & DE GENNES, P. G. 1986 Upward creep of a wetting fluid: a scaling analysis. *J. Phys. Paris* **47**, 121–127.
- KAVEHPOUR, H. P. 2003 An interferometric study of spreading liquid films. PhD. thesis, Massachusetts Institute of Technology, Mechanical Engineering Dept.
- KAVEHPOUR, H. P., OVRYN, B. & MCKINLEY, G. H. 2003 The microscopic and macroscopic structure of the precursor layer in spreading viscous drops. *Phys. Rev. Lett.* (in press).
- KOPLIK, J. & BANAVAR, J. R. 2000 Molecular simulations of dewetting. *Phys. Rev. Lett.* **84**, 4401–4404.
- KOPLIK, J., BANAVAR, J. R. & WILLEMSSEN, J. F. 1989 Molecular dynamics of fluid flow at solid surfaces. *Phys. Fluids A* **1**, 781–794.
- MILCHEV, A., MILCHEV, A. & BINDER, K. 2002 Nanodroplets on a solid plane: wetting and spreading in a Monte Carlo simulation. *Comput. Phys. Commun.* **146**, 38–53.
- ROWLINSON, J. S. & WIDOM, B. 1982 *Molecular Theory of Capillarity*. Clarendon.
- TANNER, S. H. 1979 The spreading of silicone oil drops on horizontal surfaces. *J. Phys. D: Appl. Phys.* **12**, 1473–1484.
- THOMPSON, P. A., BRINCKERHOFF, W. B. & ROBBINS, M. O. 1993 Microscopic studies of static and dynamic contact angles. *J. Adhesion Sci. Technol.* **7**, 535–554.
- THOMPSON, P. A. & ROBBINS, M. O. 1989 Simulations of contact-line motion: Slip and the dynamic contact angle. *Phys. Rev. Lett.* **63**, 766–769.
- TROIAN, S. M., HERBOLZHEIMER, E., SAFRAN, S. A. & JOANNY, J. F. 1989 Fingering instabilities of driven spreading films. *Europhys. Lett.* **10**, 25–30.
- VOINOV, O. V. 1976 Hydrodynamics of wetting. Translated from *Izv. Akad. Nauk SSSR, Mekh. Zhid. i Gaza* **5**, 76–84.
- YANG, J., KOPLIK, J. & BANAVAR, J. R. 1991 Molecular dynamics of drop spreading on a solid surface. *Phys. Rev. Lett.* **67**, 3539–3542.